DOI 10.1007/s10946-015-9503-2
Journal of Russian Laser Research, Volume 36, Number 3, May, 2015

MICROTEXTURES INDUCED BY NANOSECOND LASER ON Ni–Co ALLOY COATINGS

He Haidong,[1]* Yang Haifeng,[2] Zhou Longpeng,[2] and Chen Tianchi[2]

[1] *College of Mechanical & Electrical Engineering*
Nanjing University of Aeronautics and Astronautics
Nanjing, 210016, China

[2] *College of Mechanical & Electrical Engineering*
China University of Mining and Technology
XuZhou, 221116, China

*Corresponding author e-mail: hhdcumt @ 126.com

Abstract

Ni–Co alloys have a wide range of applications in various fields owning to their excellent physical, chemical, and mechanical properties. In this paper, we prepare Ni–Co alloy coatings on 316L stain steel surfaces by electroplating. We present a novel approach utilizing a nanosecond laser to induce microtextures on Ni–Co alloy coatings. We study experimentally the effects of laser power and scanning rate on the surface morphologies of Ni–Co alloy coatings. The results indicate that the shape and size of induced microtextures can be controlled by the laser power and scanning rate. The size of grains increases with increase in the work current of the laser (WCL) at a certain scanning rate. With the WCL constant, the size of grains decreases with increase in scanning rate while their average height increases. It is a simple and easily-controlled method for the fabrication of microstructures on Ni–Co alloy coatings, which has promising applications in investigations of the properties of microtextured surfaces, such as friction, adhesion, and wetting.

Keywords: microtextures, nanosecond laser for inducing microtextures, Ni–Co alloy, electrodeposition.

1. Introduction

Ni–Co (nickel and cobalt) alloys have become important engineering materials owning to their excellent physical, chemical, and mechanical properties. Previous investigations indicated that Ni–Co alloy coatings prepared by simultaneous code position of nickel and cobalt cations showed better corrosion resistance in comparison with Ni coatings [1–6]. Wang et al. [1] obtained Ni–Co alloy coatings with different compositions and microstructures by electrodeposition. They found that the Co content had a great influence on the composition, surface morphology, phase structure, hardness, and tribological properties. Babak et al. [2] observed that the Co content in Ni–Co alloy coatings increases due to an anomalous behavior by increasing the cobalt concentration in the electrolyte.

Sheng et al. [6] electrodeposited Ni–Co alloy coatings onto carbon steel substrates with the aid of ultrasound and investigated the effects of the ultrasound frequency on their roughness, hardness, and corrosion resistance. The results indicated that ultrasound agitation helped to decrease the roughness and enhance the hardness and corrosion resistance of the Ni–Co coatings. Ni–Co alloy coatings with low Co content have the advantages of smooth and low porosity, which can be used as functional coatings.

Manuscript submitted by the authors in English first on October 19, 2014 and in final form on May 25, 2015.
 1071-2836/15/3603-0292 ©2015 Springer Science+Business Media New York

Since the Co content is below 40%, the Ni–Co alloy coatings are highly rigid, corrosion-resisting, and wear-resisting [7]. Ni–Co alloy coatings with high Co content have magnetic coercivity, which has been used in the computer, aerospace, and electronic industry [8, 9].

Functional microstructures have great advantages in many fields of science, which has attracted considerable interest over the last decades. Solid surfaces can be microstructured by ultrashort laser pulses, as electronic excitation is faster than the heat transport by lattice vibrations [10]. According to previous investigations, many kinds of microstructures have been induced by laser treatment on various material surfaces. Ma et al. [11] investigated the surface morphological evolution of Zr-based metallic glass ablated by femtosecond lasers. Three types of permanent ring structures with microlevel spacing were obtained. Her et al. [12] found that silicon surfaces can develop arrays of sharp conical spikes when they are irradiated with 500 fs laser pulses in SF_6. The height of sharp conical spikes decreases with increase in the pulse duration or decrease in the laser fluence. Guo [13] reported on the laser-induced periodic structure with different spatial characteristics on the surface of polished ZnO single crystals upon irradiation by high-repetition-rate femtosecond laser pulses.

Korolkov et al. [14] produced nanostructures on Ni/Cu bilayer foils using a high-power femtosecond laser with a wavelength of 744 nm in different media, including air, distilled water, reagent-grade ethanol, and benzine. The results showed that surface nanostructures obtained in air and water are mostly in the form of quasiperiodic ripples with a characteristic period of 400–450 and 270–900 nm, respectively, whereas the nanostructures produced in ethanol and benzine are in the form of spikes, typically spaced 400–700 nm apart. Ionin et al. [15] obtained two separate sets of microcones on the titanium surface under various ablatives at 248 nm femtosecond-laser exposures near rough spallation crater edges and in crater centers, respectively.

Yet few studies have been published so far in whatever sources for investigations using a laser to modify the surface of Ni–Co alloy coatings.

In this paper, we prepare Ni–Co alloy coatings on the surface of stain steel substrates by electroplating. We present a novel approach utilizing a nanosecond laser to induce microtextures on Ni–Co alloy coatings. We investigate experimentally the effects of laser power and scanning rate on the surface morphologies of Ni–Co alloy coatings. Our aim is to develop an easily controlled laser-based technology for the fabrication of microtextures on Ni–Co alloys.

2. Experimental Apparatus and Process

2.1. The Electroplating Process

A schematic diagram of the electroplating setup is shown in Fig. 1, wherein the electroplating parameters were controlled by a electrochemical workstation (CHI660D). The electroplating process was carried out in a glass breaker with parallel electrodes positioned vertically inside the plating solution. The plating solution consisted of cobalt sulfate (30–80 g/l), nickel sulfate (250 g/l), nickel chloride (40 g/l), boric acid (35 g/l), sodium dodecyl sulfate (SDS), and 1,4-butynediol. SDS was used to decrease the surface tension of the plating solution. It could reduce or remove the pinholes on the electroplated coating, which were caused by the hydrogen remaining on the surface of the cathode. The pH of the plating solution was kept between 3.5 and 4.5, adjusted with boric acid.

A pure nickel plate with dimensions 180×80×10 mm was used as the anode. A 316L stainless steel substrate with dimensions 20×10×2 mm served as the cathode. Prior to the electroplating process, the

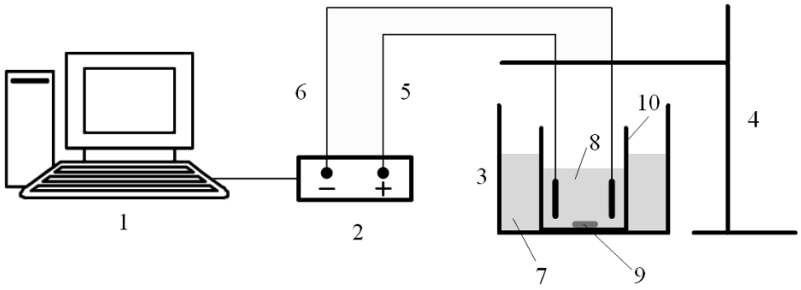

Fig. 1. Schematic diagram of the electroplating setup: computer 1, electrochemical workstation 2, magnetic stirring heating device 3, retort stand 4, positive pole 5, negative pole 6, water area 7, plating solution 8, magnetic rotor 9, and glass breaker 10.

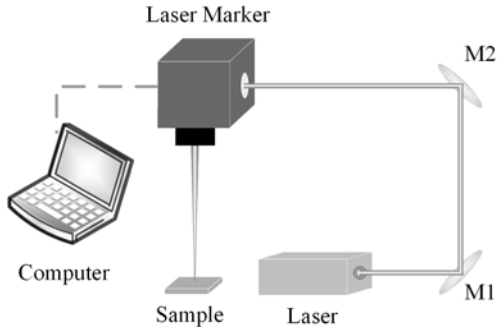

Fig. 2. Optical layout of the laser-processing system.

substrate was sequentially polished with 200–400 grit silicon carbide sandpaper and cleaned with acetone for 5 min in an ultrasound bath. Thereafter, it was activated for 1 min in 17% HCl solution at room temperature and cleaned by deionized water repeatedly. In addition, the plating solution was stirred for 20 min by a magnetic stirrer to ensure the uniform distribution of solutes in the plating solution. In all experiments, the temperature of the plating solution was confined to 55° by an automatic thermostat.

2.2. Laser Process

An ultraviolet laser (DSH-355-10, Photonics Industries, USA) with a working wavelength of 355 nm was applied to irradiate the Ni–Co alloy coatings. The intensity distribution of the output laser beam is Gaussian with a repetition rate of 10 kHz and a pulse energy of 1 mJ. The time duration of laser pulses is about 25 ns. Figure 2 shows the optical layout of the laser-treatment system. The laser beam is raised in the vertical direction by a couple of mirrors M1 and M2. After passing through a computer-controlled laser marker, the laser beam is focused onto the substrate. In laser processing, the dimension of the rectangle area scanned by the laser beam was 3×5 mm. Through repeated experiments, the scanning space was determined to be 0.01 mm.

3. Results and Discussion

3.1. Impact of the Laser Power

In this section, we describe how the Ni–Co alloy was electroplated on the substrate by choosing a current density of 25 mA/cm^2. The laser-beam power was related to the work current of the laser (WCL). For convenience, the power of the laser beam was characterized by WCL, the range of which was experimentally optimized from 33.05 to 34.50 A. The laser scanning rate (LSR) controlled by the laser marker was kept constant at 1.0 in/s. The surface morphology of Ni–Co alloy coatings was examined by scanning electron microscopy (SEM) and atomic force microscopy (AFM). The composition and content of Ni–Co coating surfaces irradiated with different WCL were measured by EDS.

Table 1 shows that the laser process does not change the type and content of elements of the Ni–Co coatings. Figure 3 a and b shows the typical surface morphology of the Ni–Co alloy coating not irradiated with the nanosecond laser. The AFM image with a dimension of 20×20 μm (Fig. 3 b) indicates that the surface morphology of the Ni–Co alloy coating is pyramidal with uneven distribution. The number and

average size of grains are 1,312 and 444.4 nm, respectively. Figure 3 c–f shows the surface morphologies of Ni–Co alloy coatings irradiated with different WCL. When the WCL was less than 33.20 A, the influence of laser power on the surface morphology of the Ni–Co alloy coating was not obvious. As the WCL increases to 33.30 A, the shape of grains shown in Fig. 3 c and d differs from that shown in Fig. 3 a and b. The number of grains decreases to 582, and the average size increases to 672.6 nm. When the WCL was 34.0 A, microtextures on the surface of the Ni–Co alloy coating disappear, and the region irradiated by the laser beam was almost smooth, as shown in Fig. 3 e. The induced microtextures (Fig. 3 f) appear again at a WCL of 33.75 A, but their shape differs from that shown in Fig. 3 a and c.

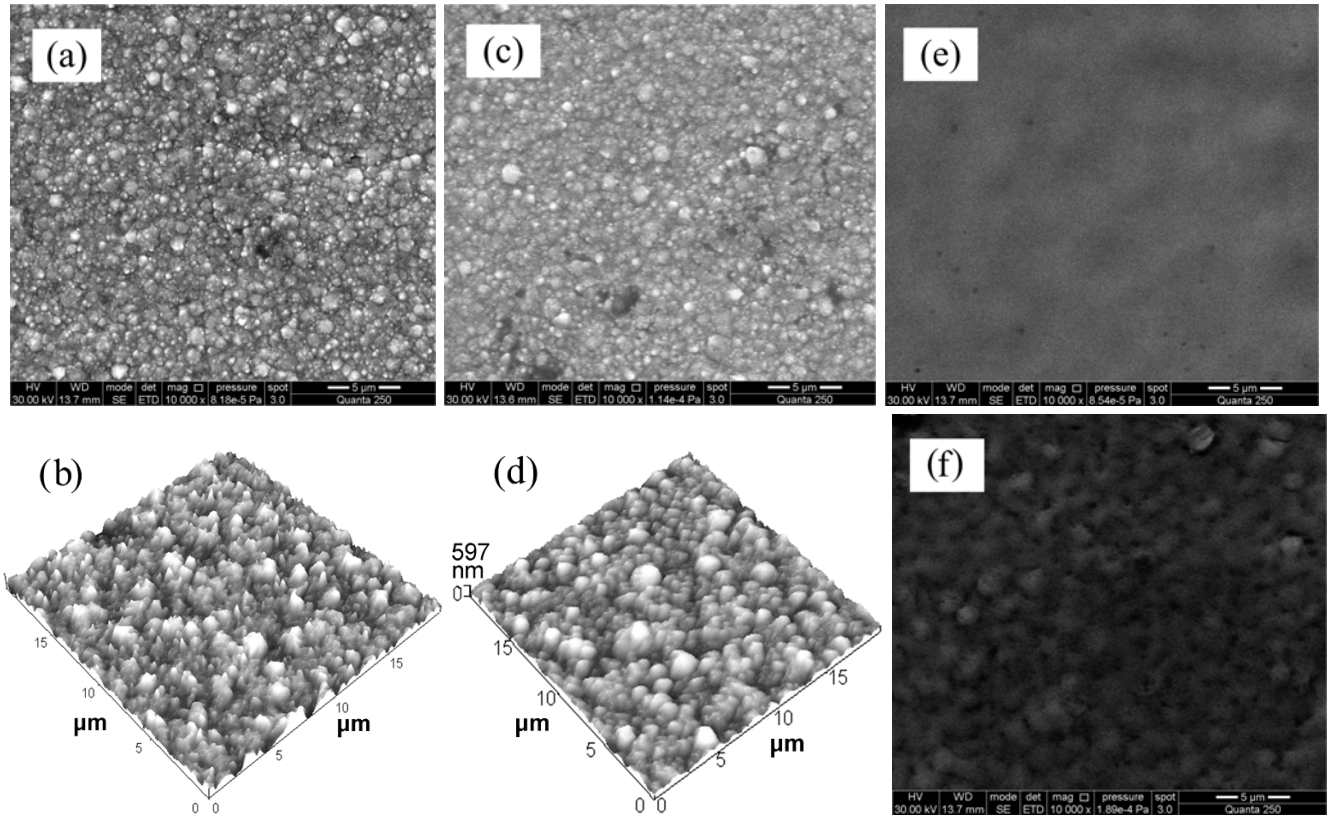

Fig. 3. The SEM and AFM images of Ni–Co alloy coatings irradiated by a laser beam with different WCL: nonirradiated surface (a, b), WCL = 33.30 A (c, d), 34.0 A (e), and 33.75 A (f).

Adjusting the WCL to 33.35 A, we obtained relatively regular microtextures on the surface of the Ni–Co alloy coating. The distribution of grains was uniform and their sizes were approximately equal, as shown in Fig. 4 a and d. The shape of grains shown in Fig. 4 d is similar to a hemisphere, and their average size was about 760.3 nm. As the WCL increased to 33.45 A, some of the gains merged. The shape of the induced microtextures looked like hemiellipsoids, as shown in Fig. 4 b and e. The average size of grains increased to 791.5 nm. Figure 4 c and f shows the surface morphologies of Ni–Co alloy coatings irradiated by the laser beam at a WCL of 33.55 A; here, the average size of grains is 884.8 nm. The experimental results indicated that the laser power has a great impact on the surface morphology of the Ni–Co alloy coating. The shape of induced microtextures is changed with WCL, and their average size increases with increase in the WCL.

Table 1. Composition and Content of the Ni–Co Coating Surfaces Irradiated at Various WCL.

WCL (A)	Nickel (%)	Cobalt (%)	Carbon (%)	Iron (%)
0.00	46.63	35.93	15.64	1.80
33.30	50.80	37.50	9.62	1.08
33.35	47.04	38.78	12.07	2.12
33.45	47.94	39.38	10.59	2.09
33.55	49.79	38.44	9.81	1.96
33.65	50.05	38.35	10.00	1.59
33.70	50.80	37.52	10.65	1.03
33.75	51.48	38.21	9.31	1.00
34.00	50.22	40.02	9.14	0.63

The laser-induced mechanism of formation of the microtextures on the surface of Ni–Co alloy coatings is not yet fully understood. We presented some possible interpretations [13, 16, 17]. When the irradiated laser fluence exceeded the melting threshold of the Ni–Co alloy, a microscale melt is produced within the area of the irradiated spot, where a high radial temperature gradient is formed. The radial temperature

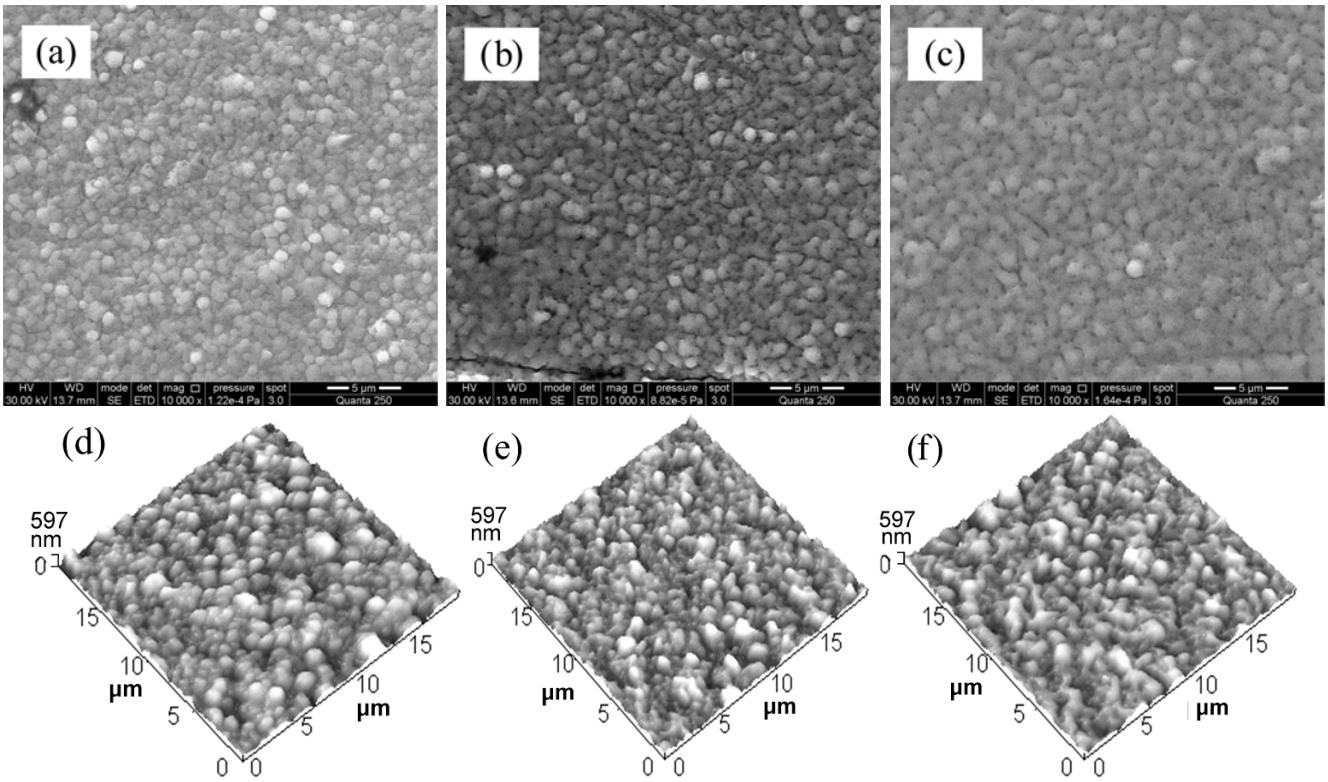

Fig. 4. The SEM and AFM images of Ni–Co alloy coatings irradiated by a laser beam with different WCL. Here, WCL = 33.35 A (a, d), 33.45 (b, e), and 33.55 A (c, f).

gradient induces a radial surface tension gradient. As the molten metal rapidly solidified from the periphery to the center, the liquid melt was expelled to the periphery of the melt by the radial surface tension gradient. As a result, hemispherical microtextures are formed on the surface of the Ni–Co alloy. With increase in the laser irradiation fluence, some microscale melt was observed to form hemiellipsoid microtextures. The repeated vaporization and redeposition also have a great influence on the formation of microtextures, but the detailed mechanism requires further investigations.

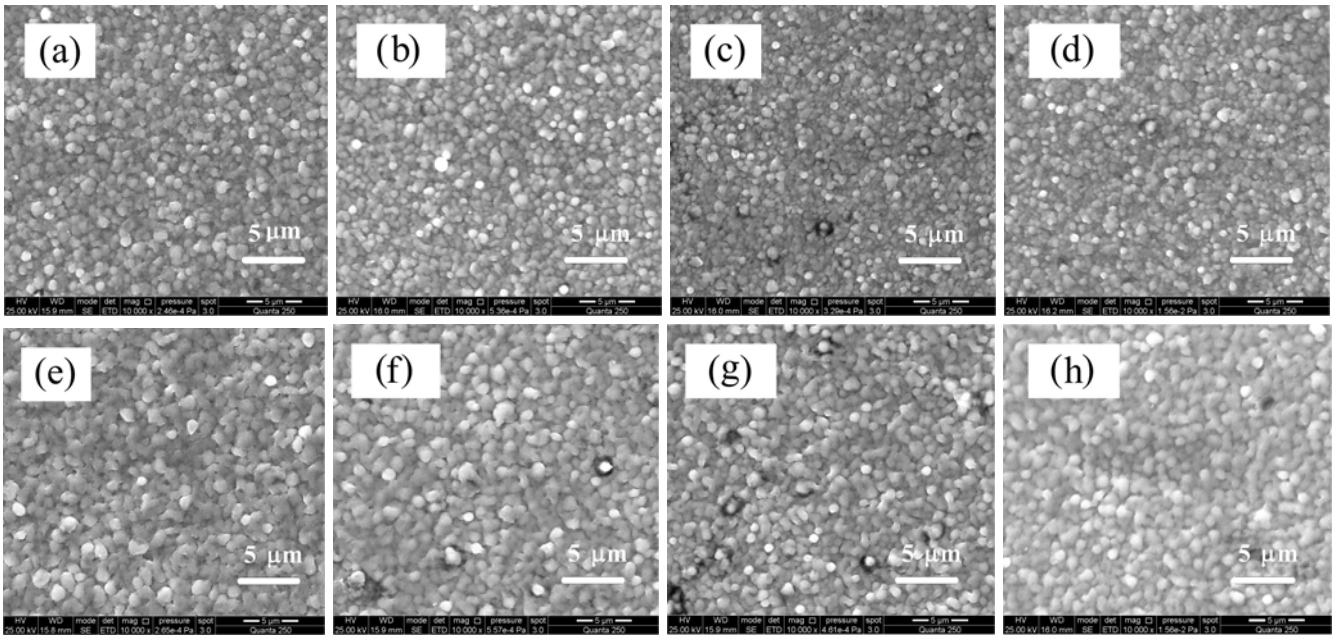

Fig. 5. SEM images of Ni–Co alloy coatings irradiated by the laser beam with different WCL and LSR. Here, WCL = 33.30 A and LSR = 0.1 in/s (a), WCL = 33.35 A and LSR = 0.5 in/s (b), WCL = 33.35 A and LSR = 1.0 in/s (c), WCL = 33.35 A and LSR = 2.0 in/s (d), WCL = 33.40 A and LSR = 0.1 in/s (e), WCL = 33.45 A and LSR = 0.5 in/s (f), WCL = 33.45 A and LSR = 1.0 in/s (g), and WCL = 33.45 A and LSR=2.0 in/s (h).

3.2. Impact of Laser Scanning Rate

In this section, we present the results of experimental studies of the influence of laser scanning rate (LSR) on the surface morphologies of Ni–Co alloy coatings. The Ni–Co alloy was electroplated on the substrates by pulse electrodeposition with the a duty cycle equal to 0.5. The experiments were conducted at various LSR of 0.1, 0.5, 1.0, and 2.0 in/s. By adjusting the WCL, both hemisphere and hemiellipsoid microtextures were obtained at different LSR. At a WCL of 33.30 A, hemisphere microtextures formed on the Ni–Co alloy coating surface (Fig. 5 a) only at a LSR of 0.1 in/s. By increasing the WCL to 33.35 A, hemisphere microtextures were produced at a scanning rate of 0.5, 1.0, and 2.0 in/s, as shown in Fig. 5 b–d. When the WCL was set to 33.40 A, hemiellipsoid microtextures (Fig. 5 e) appeared at a LSR of 0.1 in/s. In order to produce hemiellipsoid microtextures on the Ni-Co alloy surface at a LSR of 0.5, 1.0, and 2.0 in/s, the WCL must reach 33.45 A (the SEM images are shown in Fig. 5 f–h).

Figure 6 indicates that the average size of grains decreases with increase in LSR, and their average height increases with increase in LSR at constant WCL. With increase in the LSR, solidification of

molten metal increases, and the period of repeated melting-solidification process decreases. In addition, both instantaneous absorbed energy and interaction time decrease with increase in the LSR, leading to incomplete crystallization and smaller size of microtextures.

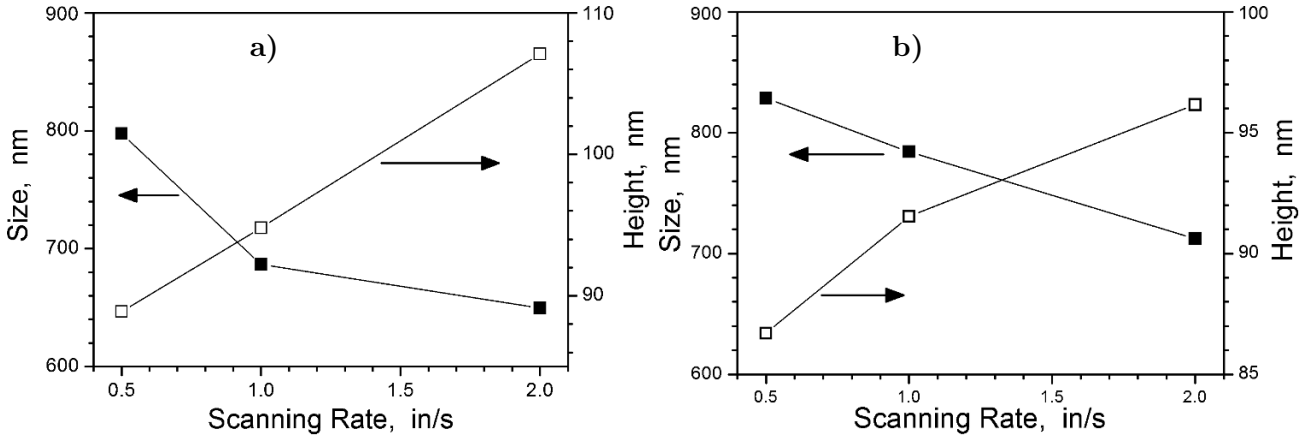

Fig. 6. The size and height of textures on the Ni–Co alloy coating surfaces induced by a laser with different WCL and LSR. Here, hemispherical microtextures (a) and hemiellipsoid microtextures (b).

4. Conclusions

In this paper, we investigated the fabrication of microtextures on Ni–Co alloy coatings by a nanosecond laser. Microtextures with various shapes and sizes were produced on the surface of the Ni–Co alloy coatings. From the presented experimental results and discussion, we draw the following conclusions:

1. The laser power has a great impact on the surface morphology of the Ni–Co alloy coating. The shape of the produced microtextures changes with the WCL, and their average size increases with increase in the WCL.

2. The average size of grains decreases with increase in the scanning rate, while their average height increases with increase in the scanning rate.

3. We elaborated a simple and easily-controlled method for the fabrication of microstructures on Ni–Co alloy coatings, which has promising applications in investigations of the properties of microtextured surfaces, such as friction, adhesion, and wetting.

Acknowledgments

The authors gratefully acknowledge the Natural Science Foundation of China (NSFC 51105360 & 51205394), the Natural Science Foundation of Jiangsu Province (Project No. BK2011218), China Postdoctoral Science Foundation Funded Projects Nos. 2012T50522 & 2011M500966, the Tribology Science Fund of the State Key Laboratory of Tribology (SKLTKF10B06), and the Fundamental Research Funds for the Central Universities under Grant 2012QNA25 for supporting this work.

References

1. Liping Wang, Yan Gao, Qunji Xue, et al., *Appl. Surf. Sci.*, **242**, 326 (2005).
2. B. Bakhit, A. Akbari, F. Nasirpouri, and M. G. Hosseini, *Appl. Surf. Sci.*, **307**, 351 (2014).
3. X. Yang, Q. Li, S. Zhang, et al., *J. Solid State Electrochem.*, **14**, 1601 (2010).
4. B. Bakhit and A. Akbari, *J. Coat. Technol. Res.*, **10**, 285 (2013).
5. B. Bakhit and A. Akbari, *Surf. Coat. Technol.*, **253**, 76 (2014).
6. M. Sheng, C. Lv, L. Hong, et al., *Acta Metall. Sin. (Engl. Lett.)*, **26**, 735 (2013).
7. N. Fenineche, C. Coddet, and A. Saida, *Surf. Coat. Technol.*, **41**, 75 (1990).
8. H. Zhu, S. G. Yang, G. Ni, et al., *Scr. Mater.*, **44**, 2291 (2001).
9. C. A. Moina and M. Vazdar, *Electrochem. Commun.*, **3**, 159 (2001).
10. M. Straub, M. Afshar, D. Feili, et al., *Phys. Proc.*, **12**, 16 (2011).
11. Fengxu Ma, Jianjun Yang, Xiaonong Zhu, et al., *Appl. Surf. Sci.*, **256**, 3653 (2010).
12. T.-H. Her, R. J. Finlay, C. Wu, and E. Mazur, *Appl. Phys. A*, **70**, 383 (2000).
13. J. Koch, F. Korte, T. Bauer, et al., *Appl. Phys. A*, **81**, 325 (2005).
14. V. P. Korolkov, A. A. Ionin, S. I. Kudryashov, et al., *Quantum Electron.*, **41**, 387 (2011).
15. A. A. Ionin, S. I. Kudryashov, S. V. Makarov, et al., *Appl. Phys. A*, **116**, 1133 (2014).
16. F. Korte, J. Koch, and B. N. Chichkov, *Appl. Phys. A*, **79**, 879 (2004).
17. A. Y. Vorobyev and C. Guo, *Opt. Express*, **14**, 2164 (2006).